

Metal nanoparticle array waveguides: Proposed structures for subwavelength devices

Shengli Zou and George C. Schatz

Department of Chemistry, Northwestern University, 2145 Sheridan Road, Evanston, Illinois 60208-3113, USA

(Received 22 June 2006; revised manuscript received 12 August 2006; published 25 September 2006)

Taking advantage of the coherent coupling among metal nanoparticles in a one dimensional array, and using partial illumination of the array, we propose a waveguide device which can excite particles in the dark with high efficiency. These array structures enable the propagation of plasmonic excitation for hundreds of microns. The results are based on coupled dipole approximation calculations, and there are important constraints on particle size, spacing and array size to produce these effects. The simulation shows that the incident wave vector can be rotated 90° using a chain structure in which the illuminated particles are spaced by slightly larger than the wavelength and the not-illuminated particles are spaced by approximately half the wavelength. We show that the near-fields around the not-illuminated particles can be ten times higher than around the illuminated particles for appropriately chosen array structures.

DOI: [10.1103/PhysRevB.74.125111](https://doi.org/10.1103/PhysRevB.74.125111)

PACS number(s): 78.67.Bf, 41.20.Jb, 73.20.Mf, 78.70.-g

I. INTRODUCTION

The optical properties of metal nanoparticles have been of interest for nearly 150 yrs.^{1,2} Advances in modern nanotechnology have enabled precise control in the preparation of particles with specified sizes and shapes, and this makes it possible to control optical properties (plasmon excitation) such that silver particles of almost any color can be produced.³⁻⁶ Also, particles can be fabricated into one or two dimensional arrays and other patterns by such techniques as *E*-beam^{7,8} and nanosphere⁶ lithography, but here the relationship between array structure and optical properties is less well understood. However this is a topic of potentially significant interest in applications to surface enhanced Raman scattering,⁹ biosensors,¹⁰⁻¹² nanoantennas,¹³⁻¹⁵ optical filters,¹⁶ and other devices. One application that has generated much past interest is metal waveguides, where it has been suggested that chains of nanoparticles can be used to bend and control light.¹⁷⁻²¹ While there are only limited experimental studies related to this concept, Maier *et al.*¹⁸ have demonstrated the propagation of light using silver nanoparticle chains for a few hundred nm.

Much of the original interest in nanoparticle chains was directed at small particles (radius $R < 30$ nm) that were closely spaced (< 100 nm).¹⁷⁻¹⁹ Here it was found that propagation distances are short, and the ability to bend light is limited. We have recently demonstrated a number of interesting properties of chains made from large particles (> 30 nm) that are spaced by half integer multiples of the optical wavelength.^{22,23} In particular, we have reported that coherent interactions between silver particles in one or two dimensional chains can produce extremely narrow resonances in which the localized plasmons associated with each particle are coupled to photonic modes of the chain. Strong coupling between particles is observed when the chain is perpendicular both to the incident wave vector and polarization directions, and when the spacing is close to the incident wavelength. The resonance condition can also be satisfied when the particles are arranged parallel to the incident wave vector direction with spacings of about half the incident wavelength. Similar two dimensional arrays were discussed

by Carron *et al.*,²⁴ and related experiments presented by Lamprecht *et al.*,²⁵ however the most optimized structure is associated with one dimensional chains. Some of the theoretical predictions for one dimensional chains have been recently confirmed through experiments by Hicks *et al.*⁸ In addition, there is work due to Malynych and Chumanov,²⁶ and to Felidj²⁷ which shows closely related effects.

In this paper we describe a new approach to the interaction of light with particle array structures in which only a portion of the structure is directly illuminated, but emission is detected from the not-illuminated particles. By optimizing the geometries of the partially illuminated array, we have designed a nanodevice which can bend light by 90° and produce particles in the dark that are more excited than those being irradiated.

II. COMPUTATIONAL DETAILS

The coupled dipole (CD) (Ref. 28) approximation method is used in these studies. Here the polarizability of each particle is calculated using the a_1 term in Mie theory^{2,22} so radiative damping and depolarization is automatically included. Earlier calculations²² have demonstrated that higher multipoles do not influence interparticle couplings, even for $R = 50$ nm particles, provided they are well separated (by half wavelength or more). A new feature in our work is that the incident plane wave field is truncated to mimic the effect of partial illumination of the particle array. To illustrate how this works, we consider an array of N particles whose positions and polarizabilities are denoted \mathbf{r}_i and α_i , respectively. The induced polarization \mathbf{P}_i in each particle in the presence of an applied plane wave field is $\mathbf{P}_i = \alpha_i \mathbf{E}_{loc,i}$ ($i = 1, 2, \dots, N$) where the local field $\mathbf{E}_{loc,i}$ is the sum of the incident plane wave and the retarded fields of the other $N - 1$ dipoles. For a given wavelength λ , this field is

$$\mathbf{E}_{loc,i} = \mathbf{E}_{inc,i} + \mathbf{E}_{dipole,i} = E_0 \exp(i\mathbf{k} \cdot \mathbf{r}_i) - \sum_{\substack{j=1 \\ j \neq i}}^N \mathbf{A}_{ij} \cdot \mathbf{P}_j, \quad (1)$$

$$i = 1, 2, \dots, N,$$

where E_0 and $k = 2\pi/\lambda$ are the amplitude and wave vector of

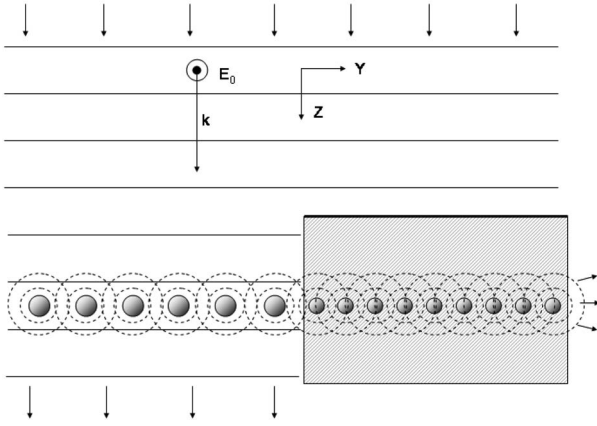


FIG. 1. Schematic of the optical excitation process being modeled. This picture shows a linear array along the Y axis that is illuminated by a plane wave whose wave vector points along Z , and whose polarization vector points along X . Particles with positive Y values are shielded from direct illumination (shaded area), but can be excited through interactions with radiation scattered from particles having negative Y values. The radiative dipolar emissions of these particles are represented by dotted circles around each particle. Note that the particles having negative Y can have a different radius and spacing than those for positive Y .

the incident wave, respectively. The dipole interaction matrix A is expressed as

$$\begin{aligned} \mathbf{A}_{ij} \cdot \mathbf{P}_j &= k^2 e^{ikr_{ij}} \frac{\mathbf{r}_{ij} \times (\mathbf{r}_{ij} \times \mathbf{P}_j)}{r_{ij}^3} \\ &+ e^{ikr_{ij}} (1 - ikr_{ij}) \frac{[\mathbf{r}_{ij}^2 \mathbf{P}_j - 3\mathbf{r}_{ij}(\mathbf{r}_{ij} \cdot \mathbf{P}_j)]}{r_{ij}^5}, \\ (i &= 1, 2, \dots, N, j = 1, 2, \dots, N, j \neq i), \end{aligned} \quad (2)$$

where \mathbf{r}_{ij} is the vector from dipole i to dipole j . Note that the first term in Eq. (2) has a $1/r$ dependence on interparticle spacing, and thus is dominant for the large array spacings we consider in this study.

In truncating the incident plane wave field, we simply omit the plane wave in Eq. (1) for those particles that are not illuminated. This implicitly assumes that the particles are shielded by a perfect absorber which prevents light from reaching those particles, does not lead to reflection or scattering, and does not interfere with the dipole interactions between the particles. Since the particles are well spaced (hundreds of nm), it is not hard to imagine shielding a selected portion of the array with an absorbing film. Previous work⁸ has demonstrated that if two chains of particles are separated by $2 \mu\text{m}$ or more, they have essentially no influence on their dipolar couplings, so we assume that the shield would have to be similarly removed from the particles.

The polarization vectors in Eq. (1) are obtained by solving $3N$ linear equations of the form

$$\underset{\sim}{\mathbf{A}} \underset{\sim}{\mathbf{P}} = \underset{\sim}{\mathbf{E}}, \quad (3)$$

where the off-diagonal elements of the matrix $\underset{\sim}{\mathbf{A}}', \mathbf{A}'_{ij}$, are the same as \mathbf{A}_{ij} , and the diagonal elements, \mathbf{A}'_{ii} , are α_i^{-1} . After

obtaining the polarization vectors, we can calculate the differential scattering cross section using

$$C_{sca} = \frac{k^4}{|E_0|^2} \sum_{j=1}^N |[P_j - \hat{n}(\hat{n} \cdot P_j)] \exp(-ik\hat{n} \cdot \mathbf{r}_j)|^2, \quad (4)$$

where \hat{n} represents the unit vector along the scattering direction, with the sum including all particles. The polarization vectors can also be used to calculate the electric field E around the particles using an expression similar to Eq. (1), but with the sum including all the particles in the array.

In our previous work, we considered the extinction spectra and near-field behavior associated with one dimensional silver nanoparticle chains,^{8,22,23,29} showing that narrow resonance lineshapes can be produced when light interacts with chains with the polarization perpendicular to the chain, and the wave vector either perpendicular or parallel to the chain. If the wave vector is perpendicular, then this leads to a resonance condition when the particle spacing is approximately an integer multiple of the wavelength, while in the parallel case, resonances are found at spacings that are a half integer multiple of the wavelength. In this paper, we use both types of resonances, again considering one dimensional chains of silver spheres. The dielectric constants of silver are from Lynch *et al.*³⁰ The particles considered in this study have a radius $R=50$ nm, which is large enough that size dependent corrections to the metal dielectric constants are unimportant.

III. RESULTS

To study near-field effects, as well as applications to waveguides that can bend the direction of propagation by 90° , we consider the electric fields $|\mathbf{E}|^2$ for a one dimensional chain of particles whose axis is perpendicular to the wave vector and polarization directions. Figure 1 presents a schematic which shows the array structure and electromagnetic fields that are involved. We assume that the chain is partially illuminated, and we examine the field that is induced in the particles that are not illuminated. We take the wave vector to define the Z axis of a coordinate system, and the polarization direction to define the X axis. The chain is taken to be perpendicular to the polarization direction, and only particles having $Y < 0$ are illuminated. In our initial calculations we consider that all the particles have the same radius and spacing, but later we will relax this assumption for reasons that will be apparent.

Figure 2 presents results for chain sizes of 401 and 801 particles. The particles have 470 nm spacings, the particle radius is 50 nm, and the incident wavelength is 470.3 nm which is slightly to the blue of the resonance wavelength 471.4 nm. Following Quinten *et al.*,³¹ we measure local intensity by determining $|\mathbf{E}|^2$ (normalized to its incident asymptotic value) 1 nm away from each particle and along the polarization direction. Figure 2 shows how this intensity declines with increasing distance from the illuminated particles. However, even at the end of the chain, i.e., $94 \mu\text{m}$ and $188 \mu\text{m}$ from the last illuminated particle for the 401 and 801 particle arrays, respectively, $|\mathbf{E}|^2$ is still larger than its incident value.

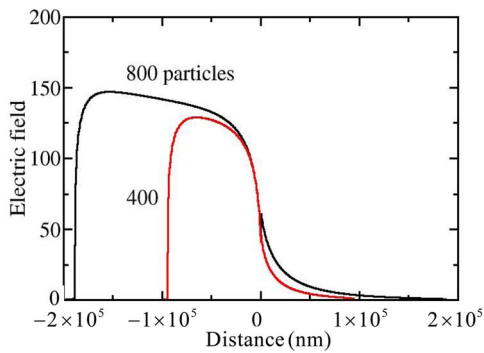


FIG. 2. (Color online) $|\mathbf{E}|^2$ versus Y for a linear array of spherical particles (50 nm radius) having 400 and 800 particles. Only particles with $Y < 0$ are illuminated.

The dependence of wave propagation on particle radius has been studied by considering $R=100$ nm. In this case, the most intense plasmonic/photonic resonance occurs when the interparticle distance is 800 nm and the incident wavelength is 800.6 nm. Calculations similar to those in Fig. 2 show that for $R=100$ nm, the intensity falls off more slowly with distance from the last illuminated particle than for the 50 nm particles. For example, for $Y=100$ μm , $|\mathbf{E}|^2$ is 9.5 while the corresponding value is 3.4 for $R=50$ nm.

Another factor that influences wave propagation is the index of the surrounding medium. To study this, we consider particles embedded in glass, for which the index of refraction is assumed to be 1.5. 801 particles with $R=50$ nm are included in the simulations with 401 particles being illuminated. The interparticle distance is taken to be 470 nm, and this leads to a resonance wavelength of 705.3 nm (roughly the spacing times the index). The calculations show that the wave amplitude decays more slowly than in vacuum. For example, for $Y=100$ μm , $|\mathbf{E}|^2$ for particle arrays in glass is 8.9 while the corresponding value is 3.4 for particle arrays in vacuum.

Note that when the array is along the Y axis, wave vector is along Z and polarization is along X , the light propagation direction in the not-illuminated region is mostly along the Y axis, i.e., perpendicular to the initial propagation direction. This means that the particle array in the not-illuminated region has the wave vector direction parallel to the array axis. In this case, one can achieve a photonic resonance in a different way than when the axis is perpendicular to the array axis, taking the spacings between particles to be *half* the wavelength. However there are also restrictions on what wavelength ranges lead to sharp resonances, and in particular sharp resonances are only found for wavelengths longer than 500 nm.⁸ For example, $R=50$ nm particles produce a sharp resonance at 510 nm with a particle spacing of 240 nm. Therefore, in order to combine this resonance in the not-illuminated region with a resonance at the same wavelength in the illuminated region, we need to use different size particles in the two regions. If we use $R=50$ nm in the not illuminated region, the desired particle size in the illuminated region is $R=60$ nm, as this gives a resonance at 513 nm for a particle spacing of 510 nm.

Based on the considerations of the preceding paragraph, an optimum efficiency waveguide has been constructed using

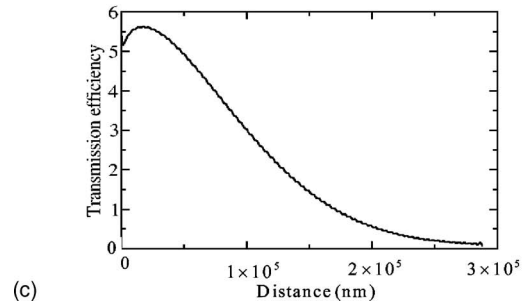
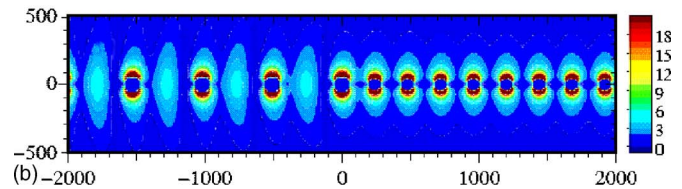
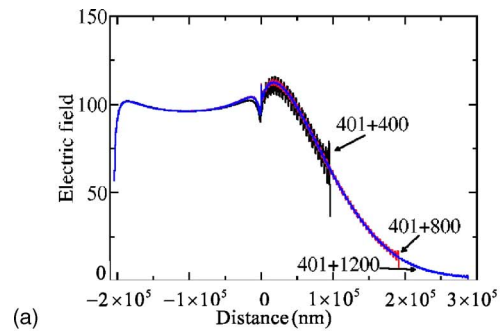


FIG. 3. (Color online) (a) $|\mathbf{E}|^2$ versus Y for a chain of 801 particles, in which the left 401 particles (those which are illuminated) have a radius of 60 nm and a spacing of 510 nm, while the right 400 particles (those not illuminated) have a radius of 50 nm and a spacing of 240 nm. (b) Electric field contour plot for particles in the chain in (a), showing particles close to the junction between the illuminated and not-illuminated particles. (c) $|\mathbf{E}_{\text{loc}}|^2$ as a function of the distance from the illuminated region.

a total of 801 particles, of which 401 particles have a radius of 60 nm, are spaced by 510 nm and are illuminated while the remaining 400 have a diameter of 50 nm, are spaced by 240 nm and are in the dark. This leads to efficient propagation of light in the dark region for a wavelength of 510.5 nm.

The results are presented in Fig. 3(a) for the same format as in Fig. 2, and also considering 401+800 and 401+1200 particle arrays. Figure 3(b) presents electric field contours for the chain with 401+400 particles. Figure 3(c) shows the local field from Eq. (1) (plotted as $|\mathbf{E}_{\text{loc}}|^2$) at the center of each particle as a function of distance from the illuminated region along the chain. This field, when compared to the incident field intensity, provides a measure of transmission efficiency of the array structure to yield light (not a near-field excitation) at each particle. This is similar to a definition used previously by Brongersma *et al.*,¹⁹ and it is a useful property for device applications as any particle can be replaced by other structures (such as semiconductor particles or nonlinear optical materials) without significantly impacting $|\mathbf{E}_{\text{loc}}|^2$.

Figure 3(a) shows that the wave can propagate for hundreds of microns with this structure. Even for distances that

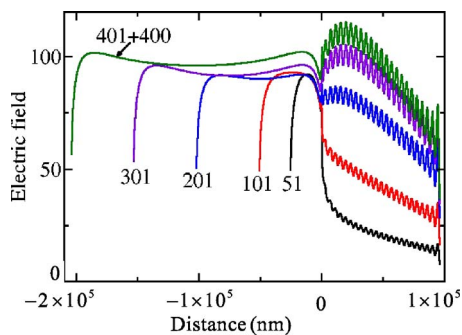


FIG. 4. (Color online) $|\mathbf{E}|^2$ associated with particles in the same chain as in Fig. 3, here showing the influence of the number of illuminated particles.

are over $100 \mu\text{m}$ from the illuminated particles, $|\mathbf{E}|^2$ is 50% of that in the illuminated particles. Increasing the number of the particles in the dark to 800 or 1200 does not change the overall picture of the energy propagation. Since 510.5 nm is close to the resonance peak wavelength of the portion of the particle arrays that are not illuminated, there is a bump in Fig. 3(a) for slightly positive Y that shows higher polarization in the not-illuminated particles than for illuminated particles. If the incident wavelength is 513 nm , this is not observed. The results in Fig. 3(c) indicate that $|\mathbf{E}_{\text{loc}}|^2$ can be enhanced by as much as a factor of 5.6 compared to the incident intensity for particle locations close to the illuminated region. In fact $|\mathbf{E}_{\text{loc}}|^2$ is greater than unity for particles that are as much as $150 \mu\text{m}$ from the illuminated region.

One issue still missing in this analysis is how many particles need to be illuminated in order to produce the behavior in Fig. 3. Figure 4 shows the energy distributions in chains with different numbers of particles illuminated. In the simulations, 400 particles with 50 nm radius and 240 nm spacings are included in the dark region, and the number of illuminated particles is varied from 51 to 401. Figure 4 shows that 400 particles are enough to make the intensity in the dark region comparable to that in the illuminated region. This is consistent with our previous studies²² showing that 400 particles are enough to converge the dipole interactions in a one dimensional chain.

We have also examined chains in which both ends are illuminated, and only particles in the center of the chain are in the dark. In the calculations, 401 particles with $R = 60 \text{ nm}$ and a 510 nm interparticle distance at each end are illuminated. The particles at the center of the chain have $R = 50 \text{ nm}$ and an interparticle distance of 240 nm . The particle numbers in the dark are varied from 100 to 400. The incident wavelength is chosen to be 510.5 nm which is optimized to generate the highest local electric fields around the particles in the dark. Peak values of $|\mathbf{E}|^2$ 1 nm away from the particle surfaces are evaluated.

Figure 5 presents results for the case where 200 particles are placed in the dark region. Here we see that the intensities for the particles in the dark are as much as 10 times those of

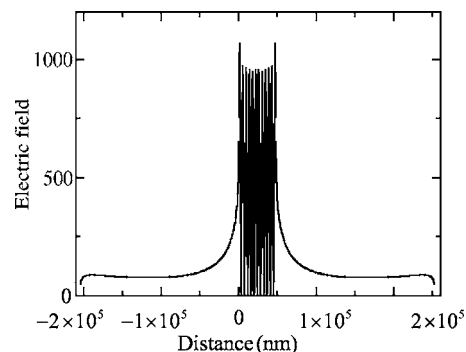


FIG. 5. $|\mathbf{E}|^2$ associated with a chain that consists of two illuminated groups of 401 particles (60 nm radius separated by 510 nm) that are spaced by a group of 200 particles (50 nm radius separated by 240 nm).

the illuminated particles. This enhancement is reduced to 7 and 6 when 100 and 400 particles are included in the center region.

IV. CONCLUSION

In summary, we have investigated the characteristics of one dimensional waveguides composed of a chain of silver particles that are partially illuminated at wavelengths where mixed plasmonic/photonic resonances may be excited. The results show that it is possible to bend the direction of propagation by 90° by suitably choosing particle size, spacing and the index of the surrounding medium. The optimized waveguide structure is a one dimensional chain that consists of different particle sizes and interparticle distances in the illuminated and not-illuminated portions of the chain. In particular, particles in the illuminated part of the chain should have a spacing that is close to the wavelength (as this produces a photonic resonance when the wave vector is perpendicular to the chain axis), while those in the not-illuminated part should have a spacing that is approximately half the wavelength (as this produces a resonance when the wave vector is parallel to the chain axis). We have also demonstrated that it is possible to design arrays in which the induced polarization in the not-illuminated particles is higher (by as much as a factor of 10) than that in the illuminated particles. These array structures should be of use in the design of plasmonic devices¹⁹ where the propagating excitation in the not-illuminated particles is manipulated and controlled, and they may also be useful for dark-field microscopy applications, including single particle sensors based on Rayleigh or Raman scattering.

ACKNOWLEDGMENTS

This work was supported by the National Science Foundation through the Nanotechnology Science and Engineering Center (NSEC), the Materials Research Science and Engineering Center (MRSEC), and by the Air Force Office of Scientific Research MURI program (F49620-02-1-0381).

- ¹M. Faraday, *Philos. Trans. R. Soc. London* **147**, 145 (1857).
- ²G. Mie, *Ann. Phys.* **25**, 377 (1908).
- ³R. C. Jin, Y. W. Cao, C. A. Mirkin, K. L. Kelly, G. C. Schatz, and J. G. Zheng, *Science* **294**, 1901 (2001).
- ⁴T. K. Sau and C. J. Murphy, *J. Am. Chem. Soc.* **126**, 8648 (2004).
- ⁵E. Hao, R. C. Bailey, G. C. Schatz, J. T. Hupp, and S. Li, *Nano Lett.* **4**, 327 (2004).
- ⁶C. L. Haynes and R. P. Van Duyne, *J. Phys. Chem. B* **105**, 5599 (2001).
- ⁷C. L. Haynes, A. D. McFarland, L. Zhao, R. P. Van Duyne, G. C. Schatz, L. Gunnarsson, J. Prikulis, B. Kasemo, and M. Kall, *J. Phys. Chem. B* **107**, 7337 (2003).
- ⁸E. M. Hicks, S. Zou, G. C. Schatz, K. G. Spears, R. P. Van Duyne, L. Gunnarsson, R. T. B. Kasemo, and M. Kall, *Nano Lett.*, **5**, 1065 (2005).
- ⁹D. A. Genov, A. K. Sarychev, V. M. Shalaev, and A. Wei, *Nano Lett.* **4**, 153 (2004).
- ¹⁰C. A. Mirkin, R. L. Letsinger, R. C. Mucic, and J. J. Storhoff, *Nature (London)* **382**, 607 (1996).
- ¹¹A. K. Boal, F. Ilhan, J. E. DeRoucher, T. Thurn-Albrecht, and V. M. Rotello, *Nature (London)* **404**, 746 (2000).
- ¹²A. Haes, S. Zou, G. C. Schatz, and R. P. Van Duyne, *J. Phys. Chem. B* **108**, 109 (2004).
- ¹³S. J. Oldenburg, G. D. Hale, J. B. Jackson, and N. J. Halas, *Appl. Phys. Lett.* **75**, 1063 (1999).
- ¹⁴J. R. Krenn, G. Schider, W. Rechberger, B. Lamprecht, A. Leitner, F. R. Aussenegg, and J. C. Weeber, *Appl. Phys. Lett.* **77**, 3379 (2000).
- ¹⁵P. Muhlschlegel, H. J. Eisler, O. J. F. Martin, B. Hecht, and D. W. Pohl, *Science* **308**, 1607 (2005).
- ¹⁶W. C. Tan, T. W. Preist, and R. J. Sambles, *Phys. Rev. B* **62**, 11134 (2000).
- ¹⁷S. A. Maier, P. G. Kik, and H. A. Atwater, *Appl. Phys. Lett.* **81**, 1714 (2002).
- ¹⁸S. A. Maier, P. G. Kik, H. A. Atwater, S. Meltzer, H. E., B. E. Koel, and A. A. G. Requicha, *Nat. Mater.* **2**, 229 (2003).
- ¹⁹M. L. Brongersma, J. W. Hartman, and H. A. Atwater, *Phys. Rev. B* **62**, R16356 (2000).
- ²⁰S. K. Gray and T. Kupka, *Phys. Rev. B* **68**, 045415 (2003).
- ²¹D. S. Citrin, *Nano Lett.* **5**, 985 (2005).
- ²²S. Zou, N. Janel, and G. C. Schatz, *J. Chem. Phys.* **120**, 10871 (2004).
- ²³S. Zou and G. C. Schatz, *J. Chem. Phys.* **121**, 12606 (2004).
- ²⁴K. T. Carron, W. Fluhr, M. Meier, A. Wokaun, and H. W. Lehmann, *J. Opt. Soc. Am. B* **3**, 430 (1986).
- ²⁵B. Lamprecht, G. Schider, R. T. Lechner, H. Ditlbacher, J. R. Krenn, A. Leitner, and F. R. Aussenegg, *Phys. Rev. Lett.* **84**, 4721 (2000).
- ²⁶S. Malynych and G. Chumanov, *J. Am. Chem. Soc.* **125**, 2896 (2003).
- ²⁷N. Felidj, G. Laurent, J. Aubard, G. Levi, A. Hohenau, J. R. Krenn, and F. R. Aussenegg, *J. Chem. Phys.* **123**, 221103 (2005).
- ²⁸L. Zhao, K. L. Kelly, and G. C. Schatz, *J. Phys. Chem. B* **107**, 7343 (2003).
- ²⁹S. Zou and G. C. Schatz, *Nanotechnology* **17**, 2813 (2006).
- ³⁰D. W. Lynch and W. R. Hunter, in *Handbook of Optical Constants of Solids*, edited by E. D. Palik (Academic Press, New York, 1985), p. 350.
- ³¹M. Quinten, A. Leitner, J. R. Krenn, and F. R. Aussenegg, *Opt. Lett.* **23**, 1331 (1998).